SYNAPSE 61:96–105 (2007)

Effect of a P-Glycoprotein Inhibitor, Cyclosporin A, on the Disposition in Rodent Brain and Blood of the 5-HT_{1A} Receptor Radioligand, [^{11}C](*R*)-(—)-RWAY

JEIH-SAN LIOW,* SHUIYU LU, JULIE A. McCARRON, JINSOO HONG, JOHN L. MUSACHIO, VICTOR W. PIKE, ROBERT B. INNIS, AND SAMI S. ZOGHBI
Molecular Imaging Branch, National Institute of Mental Health, Bethesda, Maryland

KEY WORDS cyclosporin A; CsA; P-glycoprotein; [^{11}C](*R*)-(−)-RWAY; 5-HT_{1A} receptors

ABSTRACT Limited brain uptake of radioligands with otherwise optimal properties for imaging brain receptors can be improved by blocking the effect of P-glycoprotein (P-gp), an efflux pump at the blood-brain barrier. Using small animal positron emission tomography (PET), we investigated how P-gp and its blockade with Cyclosporin A (CsA) affect rodent brain uptake of [^{11}C](*R*)-(−)-RWAY, a radioligand for brain 5-HT_{1A} receptors.

Brain uptake of radioactivity was compared in control and CsA-treated rats as well as P-gp knockout and wild type mice. Parent radioligand and radiometabolite in plasma and brain samples were determined at 30 min after injection of radioligand. PET binding potential (*BP*) was calculated with a reference tissue model.

P-gp knockout mice had 2.5- and 2.8-fold greater brain uptake of [^{11}C](*R*)-(−)-RWAY than wild type ones, measured by in vivo PET and ex vivo tissue sampling, respectively. Similarly, CsA increased rat brain uptake 4.9- and 5.3-fold, in vivo and ex vivo. In addition, CsA increased the plasma free fraction of [^{11}C](*R*)-(−)-RWAY in rats by 2.7-fold. Although CsA increased brain uptake in wild type mice by 2.5-fold, it had no effect on plasma free fraction in knockout animals. Three radiometabolites of [^{11}C](*R*)-(−)-RWAY were uniformly distributed in rat brain, suggesting they were inactive. CsA treatment increased brain uptake of [^{11}C](*R*)-(−)-RWAY and only one of its radiometabolites. Regional rat brain BP increased 27–70% in the CsA-treated rats and the P-gp knockout mice.

[^{11}C](*R*)-(−)-RWAY is a P-gp substrate in rat and mouse. The effects of CsA in rats are mediated by both P-gp blockade and displacement of the radiotracer from plasma proteins. Studies with wild type and knockout mice showed that CsA affected only P-gp in this species. **Synapse 61:96–105, 2007.**

INTRODUCTION

The P-glycoprotein (P-gp) transmembrane system is increasingly recognized as an important modulator of the disposition of therapeutic drugs and radiopharmaceuticals (Ambudkar et al., 1999). P-gp is a member of the ATP-binding cassette (ABC) family and is present in many organs of the body, where it may block absorption (e.g., intestine), have excretory-like functions (e.g., liver and kidney), or be a part of the barrier to drug entry (e.g., testes and brain) (Ambudkar et al., 2003; Doige and Ames, 1993). P-gp and probably other ABC transporters help to create the blood-brain and the blood-central spinal fluid barriers. These transporters prevent uptake of a subset of drugs that would otherwise have lipophilicity and molecular weight appropriate to enter brain. For example, loperamide is an opiate receptor agonist with adequate lipophilicity to enter brain, and yet it has only peripheral and no central nervous system activ-

Contract grant sponsor: Intramural Research Program of NIMH; Contract grant number: Z01-MH-002795-04.

*Correspondence to: Jeih-San Liow, Ph.D., National Institute of Mental Health/National Institutes of Health, Molecular Imaging Branch, 1 Center Drive, Room B3-10, MS 0135, Bethesda, MD 20892-0135.
E-mail: liowj@mail.nih.gov

Received 18 July 2006; Accepted 27 September 2006

DOI 10.1002/syn.20348

Published online in Wiley InterScience (www.interscience.wiley.com).

ity. Although a mystery for a few decades, we now know that loperamide is an avid substrate for P-gp efflux from the brain (Dagenais et al., 2004; Passchier et al., 2003; Sadeque et al., 2000; Schinkel et al., 1996). If a PET receptor-imaging agent is a substrate for P-gp, then its brain uptake will be reduced and consequently an additional kinetic parameter must be considered in the already complicated analysis of receptor density. For instance, if a subject had reduced brain uptake of a tracer, it could not be clearly attributed to either a smaller number of receptors or a more active P-gp pump.

(*R*)-(−)-RWAY is a potent antagonist (K_i = 0.6 nM) of the serotonin subtype 1A (5-HT$_{1A}$) receptor (McCarron et al., 2004). We developed a ^{11}C-labeled version as a PET radioligand for human use. Because another 5-HT$_{1A}$ antagonist, MPPF with structure similar to RWAY, is a substrate for P-gp (Passchier et al., 2000) we tested [^{11}C](*R*)-(−)-RWAY in rodents and found that it was also a substrate for this efflux pump at the blood-brain barrier. The purpose of this study was to use [^{11}C](*R*)-(−)-RWAY as representative of a PET radioligand that is vulnerable to P-gp transport and thereby examine the effect of P-gp blockade in both brain and plasma on quantitation of the imaging results.

MATERIALS AND METHODS

Preparation and analysis of [^{11}C](*R*)-(−)-RWAY

No-carrier-added [^{11}C]iodomethane, was prepared from [^{11}C]carbon dioxide with a PET-trace Microlab device (GE Healthcare). [^{11}C](*R*)-(−)-RWAY was obtained in a coupled Auto-loop apparatus (Bioscan) by treating the desmethyl precursor, (2,3,4,5,6,7-Hexahydro-1{4-[1[4-(2-Hydroxyphenyl)-piperazinyl]]-2-phenylbutyryl}-1*H*-azepine (0.3 mg) (McCarron et al., 2004) with [^{11}C]iodomethane at room temperature for 5 min in DMF (80 μl) that contained tetrabutylammonium hydroxide as base (4.5 μl; 0.167 M in methanol). [^{11}C](*R*)-(−)-RWAY was isolated by reversed-phase high-performance liquid chromatography (HPLC) on a Ultrasphere column (250 × 10 mm i.d.; particle size, 5 μm; Beckman), eluted at 6 ml/min with acetonitrile-0.1 M ammonium formate [(50:50 v/v) for 2 min, increased to 60:40 over 2 min and then maintained at 60:40 for 10 min]. The retention time was 9.4 min. The mobile phase was removed by rotary evaporation and the residue dissolved in 0.9% saline containing 5% ethanol.

Purity and specific radioactivity were determined by reversed-phase HPLC on a Prodigy column (250 × 4.6 mm i.d., particle size 10 μm; Phenomenex) eluted with acetonitrile-0.1 M ammonium formate (50:50 v/v) at 2 ml/min, with the eluate monitored for radioactivity and absorbance at 240 nm. [^{11}C](*R*)-(−)-RWAY eluted at 5.5 min.

Animal preparation

Male Sprague-Dawley rats and age-matched male and female P-gp knockout mice (*mdr-1a/1b*(−/−)) (Schinkel et al., 1994) (model 001487-MM, double homozygotes) and wild type mice (*mdr-1a/1b*(+/+)) (model FVB) were purchased from Taconic Farm (Germantown, NY). All animal experiments were performed in accordance with the Guide for Care and Use of Laboratory Animals and were approved by the National Institute of Mental Health Animal Care and Use Committee. Animals used in the ex vivo and in vivo experiments were anesthetized with 1.5% isoflurane in oxygen, and body temperatures were maintained at 36.5–37.0°C with a heating pad or lamp. Intravenous injections (i.v.) were performed via polyethylene cannulae (PE-10; Becton Dickinson, Franklin Lakes, NJ) in the rat penile or mouse tail vein. The cannulae were secured in place with tissue adhesive (Vetbond; 3M, St. Paul, MN). CsA (100 mg, Sigma-Aldrich, Milwaukee, WI) was dissolved in ethanol (440 μl) followed by the addition of Cremophor EL, (850 mg, BASF, Ludwigshafen, Germany) for a final concentration of 75 mg/ml. Rats and P-gp knockout mice were treated with CsA (50 and 25 mg/kg i.v., respectively) 30 min before injection of the radioligand.

Rat and mouse brain imaging studies

Rodent imaging was performed with the Advanced Technology Laboratory Animal Scanner (ATLAS). This small animal PET camera has an effective transaxial and axial field-of view of 6.0 and 2.0 cm, respectively (Seidel et al., 2003). A single rat or a P-gp knockout and paired wild type mouse were placed in the camera gantry and administered a bolus injection of radioligand (Table I). The injected radioactivity was determined based on (1) the linear range of scanner performance, i.e., <300,000 per s singles rate and (2) <10% receptor occupancy. Serial dynamic scans began at the time of injection and continued for 100 min with frames of 6 × 20 s, 5 × 1 min, 4 × 2 min, 3 × 5 min, 3 × 10 min and 2 × 20 min. Data were corrected for random events and detector efficiency. Images were reconstructed by a 3D ordered-subset expectation maximization algorithm into 17 coronal slices with 3 iterations and 16 subsets, resulting in a resolution of approximately 1.6 mm full width at half maximum (Johnson et al., 2002; Liow et al., 2003). The reconstructed voxel size was 0.56 × 0.56 × 1.12 mm. No attenuation or scatter correction was applied.

Tomographic images were analyzed with pixel-wise modeling computer software (PMOD Group; Zurich, Switzerland). Regions of interest (ROIs) were drawn on coronal slices guided by a rat brain stereotaxic atlas (Paxinos and Watson, 1998). The ROIs included forebrain, frontal cortex, occipital cortex, hippocampus, and cerebellum. Similar approach was taken in the case of the mouse where guidance by a mouse brain atlas (Paxinos and Franklin, 2001) was utilized.

TABLE I. Animal and study information

Treatment	Species	*n*	Weight	Administered doses	
				Radioactivity (MBq)	Mass (nmol/kg)
Imaging studies					
Control	Rat	3	320 ± 27	38.0 ± 5.9	3.4 ± 2.1
CsA	Rat	4	381 ± 121	34.9 ± 8.6	2.8 ± 1.2
Wild type	Mouse	3	27.8 ± 5.1	23.5 ± 9.9	14.9 ± 4.1
P-gp knockout	Mouse	3	26.7 ± 1.9	16.7 ± 6.0	15.2 ± 6.6
CsA wild type	Mouse	3	32.8 ± 1.9	12.1 ± 1.4	10.7 ± 1.6
CsA P-gp knockout	Mouse	3	27.5 ± 2.4	12.9 ± 1.7	8.6 ± 2.7
Ex vivo studies					
Control	Rat	3	321 ± 23	54.0 ± 13.3	3.7 ± 1.3
CsA	Rat	3	282 ± 28	54.2 ± 11.4	6.2 ± 1.5
Wild type	Mouse	4	30.1 ± 4.9	12.5 ± 7.9	14.2 ± 8.3
P-gp knockout	Mouse	4	23.9 ± 2.2	11.2 ± 5.8	17.1 ± 11.0

Brain uptake of radioactivity was decay corrected to injection time and expressed as percent standard uptake value (%SUV), which normalizes for injected radioactivity and body weight.

%SUV = [(radioactivity per g tissue)/injected radioactivity] × g body weight × 100.

To quantify 5-HT_{1A} receptor density, we used a two-parameter multi-linear reference tissue model (MRTM2) (Ichise et al., 2003), with cerebellum as the reference region. This method estimates *BP* (which is proportional to receptor density) and blood flow of the region relative to cerebellum (R_1). To assess the specific binding after CsA treatment, a displacement study was performed in CsA-treated rats with i.v. injections of WAY 100635 (2.0 mg/kg, Axon Bio Chemicals, The Netherlands) at 20 min after radioligand injection.

Measurement of parent and radiometabolites in plasma and brain

Thirty minutes after injecting the radioligand, anticoagulated blood samples (2 ml) were obtained by cardiac puncture. The animals were then sacrificed immediately by decapitation and brain tissue processed as described below. The plasma samples (300 μl) were isolated from whole blood with centrifugation at 1800*g* for 3 min (Model 426, Thermo IEC; Needham Heights, MA) and placed in acetonitrile (700 μl) spiked with standard (*R*)-(−)-RWAY (20 μg) and mixed well. Water (100 μl) was then added to the plasma-acetonitrile samples and mixed again. The total radioactivities were measured in a calibrated γ-counter with an electronic window set between 360 and 1800 keV (counting efficiency, 51.9%) (Model 1480 Wizard; Perkin-Elmer, Boston, MA).

The brain was resected, weighed, placed in acetonitrile (0.5–1.0 ml spiked with 50 μg (*R*)-(−)-RWAY), and then measured in the γ-counter. Brain tissues were then homogenized (Tissue Tearor, Model 985-370; Bio-Spec Products, Bartlesville, OK) and again after the addition of water (9% of its tissue-acetonitrile volume). The homogenizer was decontaminated between samples with three washes of acetonitrile. Samples were centrifuged at 9400*g* for 1 min (Allegra™ 21R, Beckman Coulter Inc., Palo Alto, CA). γ-Counter measurements were taken to monitor the acetonitrile extraction efficiency. Thus, the supernates were analyzed by HPLC and the radioactivities in the resulting precipitates were used to calculate the percent recovery of radioactivity in the acetonitrile supernates. The tissue parent and radiometabolite concentrations were calculated as the product of the radio-HPLC fractional parent or radiometabolite activity multiplied by the total tissue dpm/g. The recovery of added [^{11}C](*R*)-(−)-RWAY to plasma samples was >95%, and the recovery of total radioactivity from tissues and plasma samples was >90%.

The radioanalytical system used in these studies consisted of Beckman Gold (Palo Alto, CA) pumps in line with a photodiode-array detector and a flow-through NaI(Tl) scintillation detector/rate meter (Bioscan; Washington, DC,USA). Reverse phase chromatography was carried out on Novapak C_{18} column (100 × 8 mm^2; Waters, Milford, MA) with a radial compression module RCM-100 eluted with methanol: water: triethylamine (75:25:0.1; by volume), at 2.0 ml/min. Radio-chromatographic data were collected and stored on "Bio-Chrome Lite" software (Bioscan) and analyzed after decay correction of the radiochromatograms. The recovery of radioactivity from HPLC column was monitored either by γ-counter measurements of the eluates or by injection of absolute methanol (2 ml) at the end of a radiochromatography with continued monitoring of radioactive eluates.

The plasma free fraction (f_1) of [^{11}C](*R*)-(−)-RWAY was determined by ultrafiltration with Amicon Centrifree® units (30 K M.W. cut-off; Millipore, Milford, MA) at a centrifugal force of 3000*g* for 20 min, as previously described (Gandelman et al., 1994). The effect of CsA treatment was determined in plasma collected from a control rat and another rat at 30 min after injection of CsA (50 mg/kg).

RESULTS

Radioligand

[^{11}C](*R*)-(−)-RWAY was prepared from the desmethyl precursor with an overall decay-corrected radiochemical yield of 26.7% ± 11.8% (n = 23; mean ± SD). The

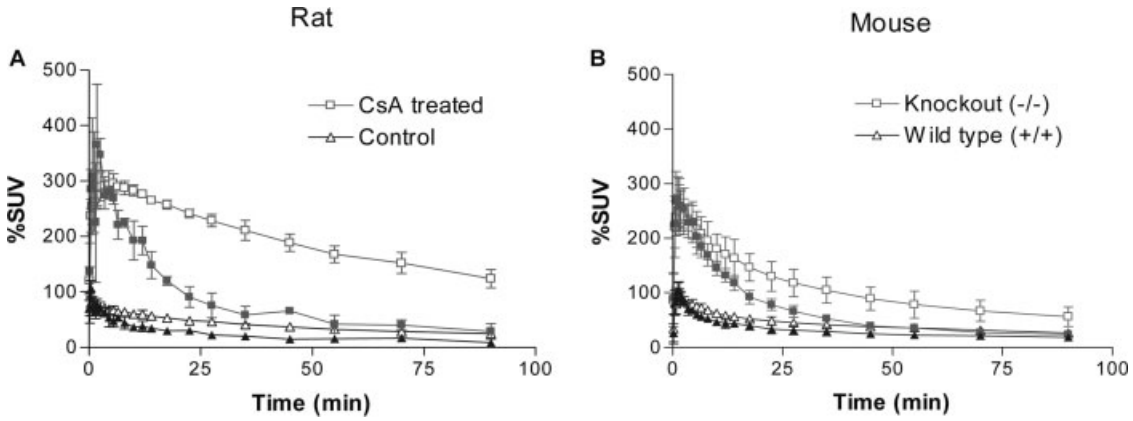

Fig. 1. Time-activity curves from PET images of [^{11}C](*R*)-(−)-RWAY in control and CsA-treated rats (**A**) and in wild type and P-gp knockout mice (**B**). Open symbols are forebrain and solid symbols are cerebellum. CsA (50 mg/kg) was administered 30 min before injection of the radioligand. Each curve is the mean ± SD %SUV from 3 animals.

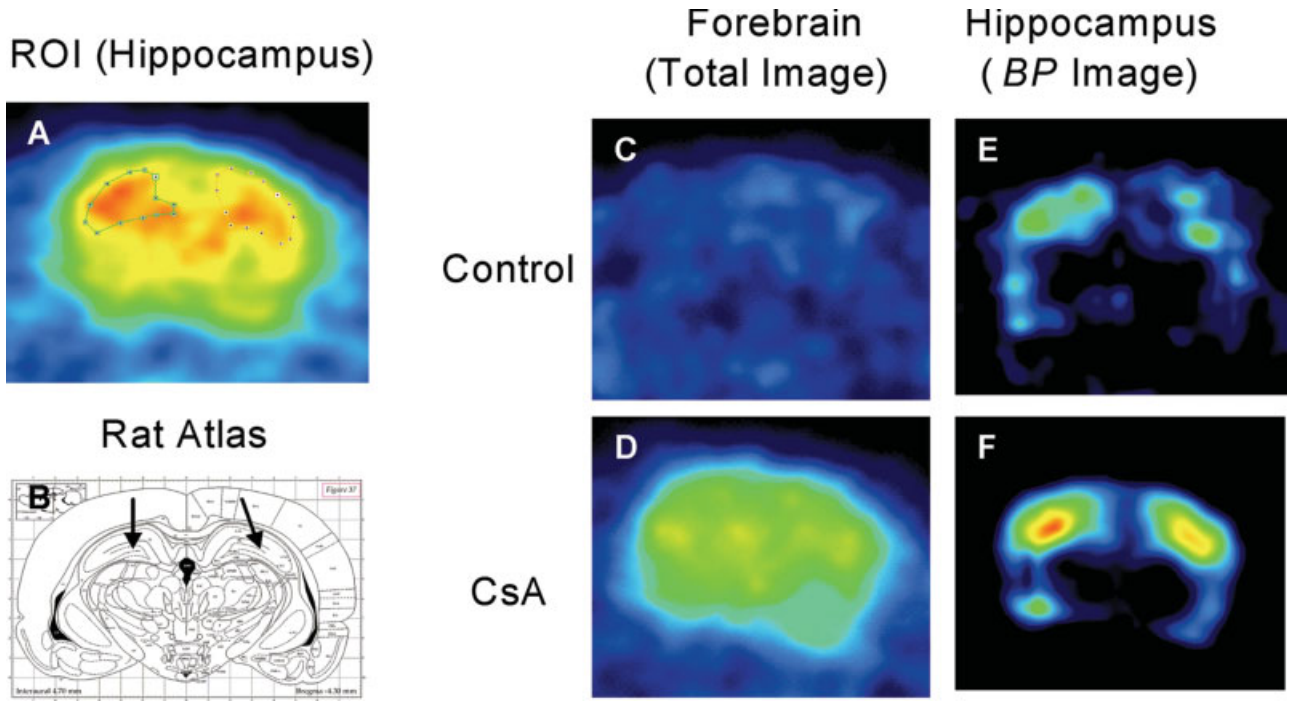

Fig. 2. Uptake of [^{11}C](*R*)-(−)-RWAY in rat brain. Regions of interest were placed on left and right hippocampi (**A**), using coronal PET images with reference to a rat brain atlas (**B**). Total uptake of radioactivity is shown in control (**C**) and CsA-treated rats (**D**). Similarly, *BP* images are shown in control (**E**) and CsA-treated animals (**F**).

radiochemical purity was 99.9% ± 0.2% (n = 23). The specific radioactivity, decay-corrected to the time of injection, was 39.1± 15.8 GBq/μmol.

Rat and mouse brain imaging studies

After administering [^{11}C](*R*)-(−)-RWAY, forebrain and cerebellar radioactivity peaked early (within one min) but was only 80 and 100% SUV in control rats (n = 3) and in wild type mice (n = 3), respectively (Figs. 1 and 2). CsA treatment caused ∼4-fold increase in peak regional rat brain uptake (n = 3), and the P-gp knockout mice had ∼2.6-fold greater uptake (n = 3) than those in the wild type animals. Peak uptake values are vulnerable to variability due to the speed of injecting the radioligand. For this reason, we assessed the effect of P-gp blockade and or its genetic inactivation using area-under-the-curves (AUC) of the plot of regional brain uptake (%SUV) vs. time for the entire duration of the scan. CsA caused a 4.9-fold increase of brain uptake in rats, and P-gp knockout mice had 2.5-fold greater uptake than wild type mice. Thus,

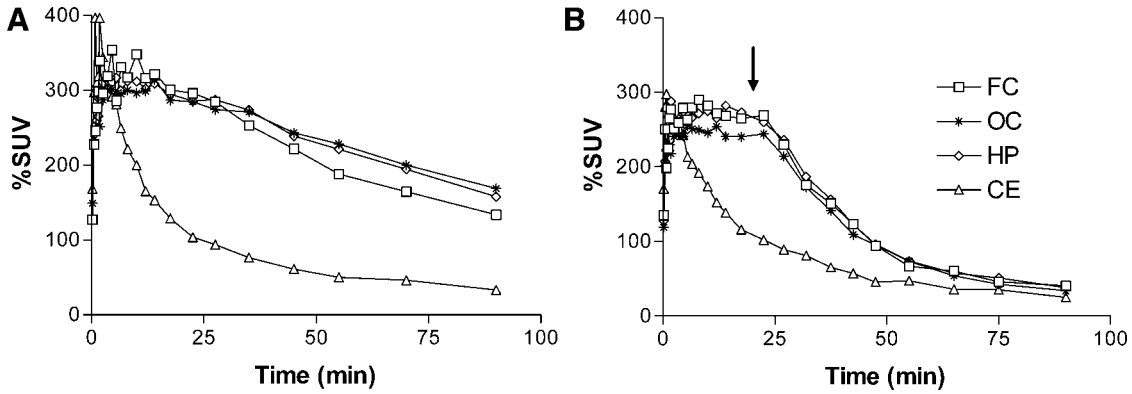

Fig. 3. Time-activity curves of [^{11}C](*R*)-(−)-RWAY in the 5HT$_{1A}$-rich (hippocampus, frontal cortex, occipital cortex) and poor (cerebellum) regions of the brain in CsA-treated rats (**A**) and when displaced at 20 min by WAY 100635 (2 mg/kg i.v.) (**B**).

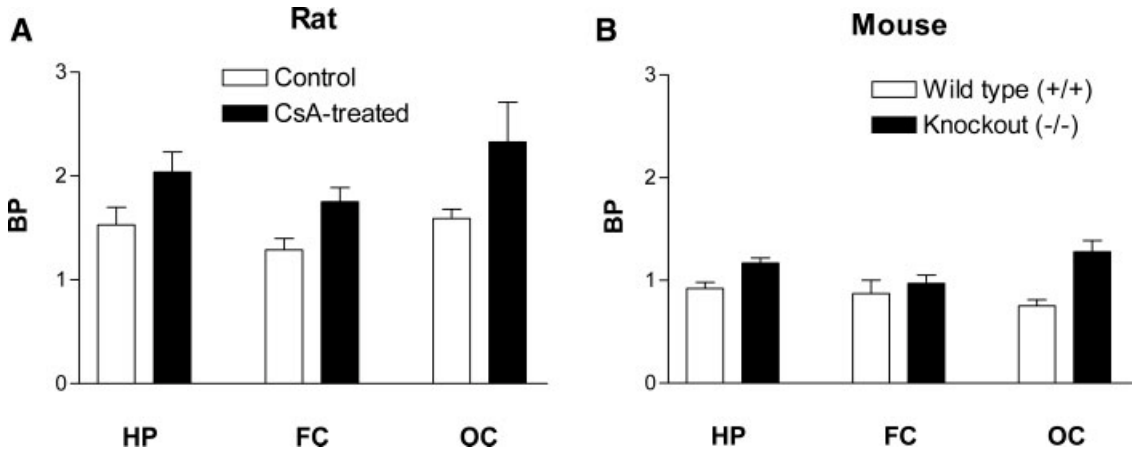

Fig. 4. Effects of CsA treatment in rats (**A**) and P-gp knockout mice (**B**) on the *BP* of [^{11}C](*R*)-(−)-RWAY in hippocampus, frontal cortex, and occipital cortex. *BP* was determined from PET image analysis with MRTM2 and using the cerebellum as the reference input.

AUC and peak brain uptake measurements showed similar effects, consistent with CsA causing a sustained blockade of P-gp during the entire scan.

In the displacement study, after CsA administration, the increased forebrain uptake of [^{11}C](*R*)-(−)-RWAY was displaced by WAY 100635 down to the nonspecific level found in cerebellum ($n = 1$, Fig. 3). This displacement suggests that the CsA-enhanced signal was parent radioligand specifically bound to 5-HT$_{1A}$ receptors rather than an inactive radiometabolite.

We used a reference tissue method to calculate pixel-wise values of *BP*, which is proportional to receptor density and equal to the ratio at equilibrium of specific to nondisplaceable uptake. Since an F test has shown that variances were equal ($P < 0.995$), a one-way analysis of variance was performed for the *BP* between control and CsA-treated rats, and between wild type and P-gp knockout mice. Results of the one-way analysis of variance demonstrated a significant effect of P-gp inactivation ($\alpha = 0.05$) in all regions except for mouse frontal cortex. The mean *BP* values in all three regions of both rats and mice (Fig. 4) ranged from 27 to 70% higher in the P-gp modulated animals than the corresponding control animals. However, 27–70%, increase in *BP* in the P-gp modulated animals was much smaller than the 2.5 to 4.9-fold uptake increase seen with the AUC. The variable increase in mean *BP* could have been caused by a differential regional brain localization of P-gp function. For example, inactivation of P-gp in rodents may have caused a relatively smaller effect in cerebellar uptake and thereby increases the regional *BP*. Thus, for radiotracers that are substrates of P-gp, reference tissue methods to estimate receptor rodents density may be vulnerable to error because of regional variation in the function of P-gp.

Use of P-gp knockout mice to assess the peripheral effects of CsA

CsA has several peripheral effects not mediated by P-gp blockade e.g., inhibition of CYP3A4 and toxicity to

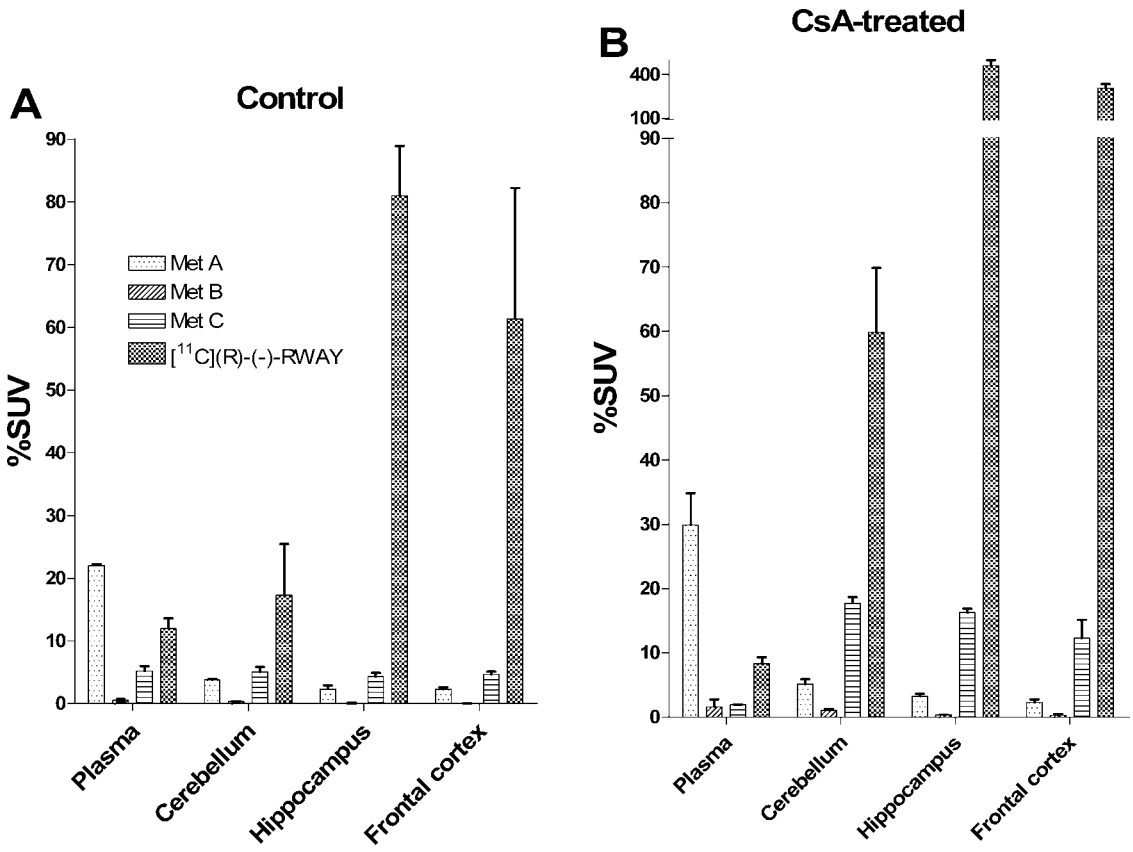

Fig. 5. Ex vivo rat plasma and regional brain distribution (%SUV) of [^{11}C](*R*)-(−)-RWAY and its three radiometabolites in control (**A**) and in CsA-treated (**B**) rats at 30 min after radioligand injection. The radioactivities were resolved into the various components with reversed phase HPLC. Each bar represents the mean of triplicate rats ± SD.

liver and kidney (Moochala and Renton, 1986; Wacher et al., 1998). We used the P-gp knockout and wild type mice to assess these peripheral effects. Using brain AUC as the outcome measure, CsA treatment increased uptake in wild type mice from 4100 ± 472 to 10,200 ± 2550 %SUV-min ($n = 3$). In contrast, CsA treatment of P-gp knockout mice had negligible effects, from 10,100 ± 2330 to 10,200 ± 2600 %SUV-min ($n = 3$). In summary, CsA treatment made the wild type mouse response similar to that of the knock-out mouse. CsA had no effect in the knock-out mouse, suggesting that it had no measurable peripheral effects on brain uptake of [^{11}C](*R*)-(−)-RWAY.

Ex vivo plasma and regional brain composition study

CsA treatment of rats caused 2.7-fold increase ($P < 0.005$) in the plasma free fraction of [^{11}C](*R*)-(−)-RWAY, from 1.21% ± 0.04% to 3.29% ± 0.40%. CsA may have displaced radioligand binding to plasma proteins and thereby made more of the radioligand available to enter brain. CsA caused 5.3-fold increase of brain uptake in rat (see above), and about half of that effect (i.e., 2.7-fold) may have been caused by the increase in plasma free fraction.

For the mice, plasma free fraction was not responsible for increased brain uptake in the P-gp knockout animals. In fact, the f_1 values in the knockout mice (1.74% ± 0.1%) were lower (about 25%) than that in wild type mice (2.31% ± 0.12%). That is, despite lower f_1 values, the P-gp knockout mice had higher brain uptake.

The ex vivo components of radioactivity and their distributions in rat brain and plasma were measured chromatographically at 30 min following the bolus injection of [^{11}C](*R*)-(−)-RWAY (Fig. 5). Three radiometabolites of [^{11}C](*R*)-(−)-RWAY were detected both in plasma and brain. These radiometabolites eluted earlier than the parent radioligand, indicating that they were less lipophilic than [^{11}C](*R*)-(−)-RWAY. Control rat forebrains contained 92.2% ± 2.5% parent and those of the CsA treated animals 95.8% ± 0.8%. In the control rats, the %SUVs of [^{11}C](*R*)-(−)-RWAY in the hippocampus, frontal cortex, and occipital cortex were 81, 61, and 55 compared to 461, 304, and 292 respectively, in the CsA-treated rats (Fig. 5B). CsA-treatment caused an average of 5.3-fold (5.0–7.0) increase of uptake in hippocampus compared to control rats (Fig. 5A). Note that the lower uptake value

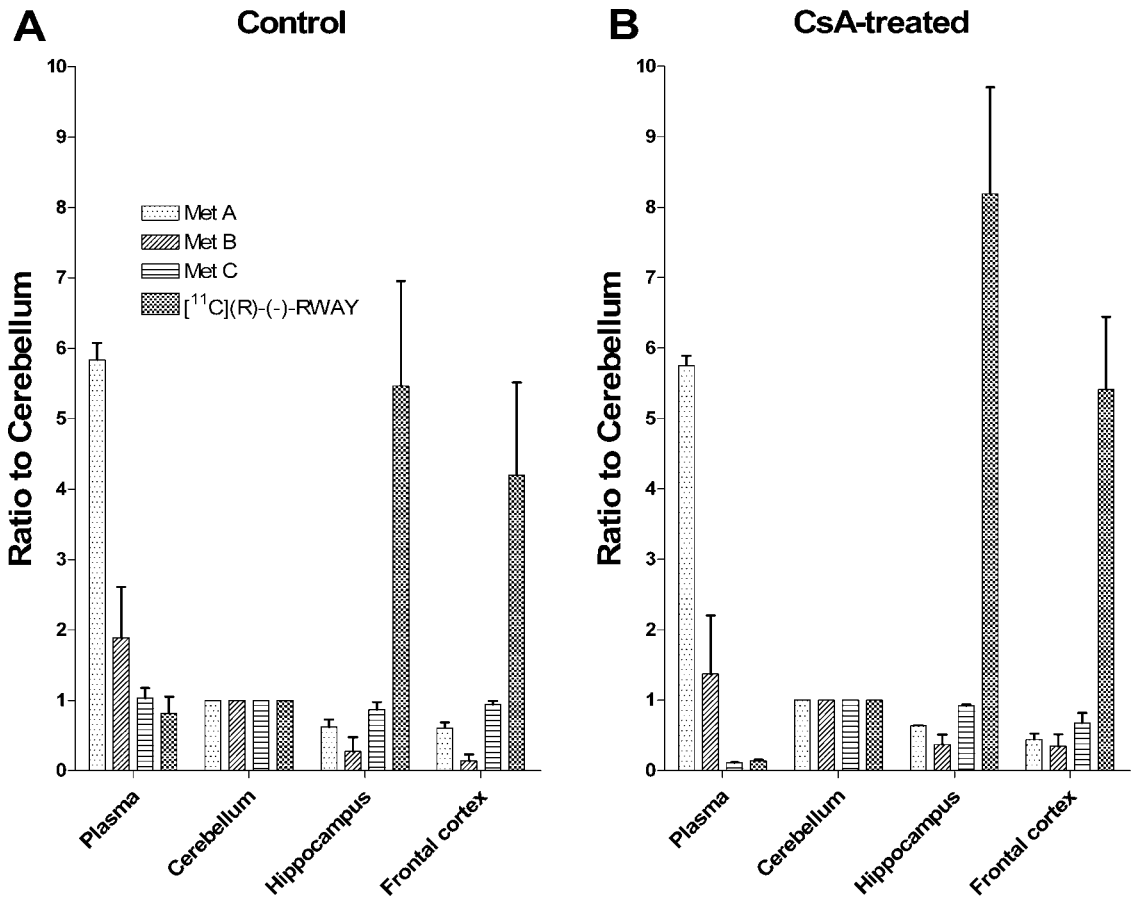

Fig. 6. Ratios of the regional brain concentration of [^{11}C](*R*)-(−)-RWAY and its radiometabolites to their cognates in the nonspecific cerebellar region in control (**A**) and CsA-treated rats (**B**) at 30 min after radioligand injection.

in hippocampus for in vivo imaging compared to ex vivo measurement is likely due to the effect of partial volume averaging exacerbated by the unique shape of hippocampus.

The ratios of tissue concentration of [^{11}C](*R*)-(−)-RWAY and of its individual radiometabolites to their cognates in the cerebellum (Fig. 6) reveal the presence or absence of 5-HT$_{1A}$ receptor-specific binding for each radiochemical species. The nonspecific distribution of the radiometabolites in all brain regions, for both groups of rats was evident by their ratio of unity. The parent radioligand ratios in the frontal cortex and hippocampus were 4.2 ± 2.3 and 5.5 ± 2.6 in the control rats (Fig. 6A) and 5.4 ± 1.8 and 8.2 ± 2.6 in the CsA-treated ones (Fig. 6B), respectively.

Radiometabolites A, B, and C were present in all brain regions and plasma, with B showing the lowest concentrations (0.0–1.1%SUV). The concentrations of these metabolites were similar among target and background regions of brain, suggesting that they are inactive (i.e., they do not bind to 5-HT$_{1A}$ receptors). Radiometabolite C had the highest concentration, which was increased 3-fold with the CsA-treatment.

We also examined the ratio of brain to plasma parent concentrations, because P-gp blockade should increase this ratio for compounds that are substrates for this transporter. The plasma concentrations of [^{11}C](*R*)-(−)-RWAY were unchanged whether the P-gp efflux pump was pharmacologically blocked in rats or genetically knocked out in mice, but the brain uptake relative to plasma was increased (Table II). The %SUV of [^{11}C](*R*)-(−)-RWAY in plasma of control (12.0 ± 1.6) and CsA-treated rats (8.3 ± 1.7) were similar, but the corresponding hippocampal %SUV values were 81 ± 8 and 461 ± 5 respectively (Table II). Thus, the brain to plasma ratio in hippocampi of CsA-treated rats was 57, compared to ∼7 in control animals. Similar trends were observed in mice, where the brain to plasma ratio of [^{11}C](*R*)-(−)-RWAY in knockout mice was 19, compared to ∼5 in wild type animals.

These ex vivo measurements from a single time point (30-min) are difficult to interpret definitely. That is, single time-point measurements are vulnerable to CsA-induced changes in the kinetics of the parent or radiometabolites and may not reflect measurements with AUC integrated throughout the studied

TABLE II. Ex vivo plasma and brain distribution of [^{11}C](R)-(−)-RWAY

Treatment	Species	%SUV [^{11}C](*R*)-(−)-RWAY		Brain/ plasma ratio
		Plasma	Brain[a]	
Control	Rat	12.0 ± 1.6	81.0 ± 8.0[a]	6.8 ± 0.3[a]
CsA	Rat	8.3 ± 1.7	461.0 ± 4.8[a]	57.0 ± 13.3[a]
Wild type	Mouse	7.1 ± 3.9	31.4 ± 13.0	5.0 ± 1.9
P-gp knockout	Mouse	5.5 ± 3.4	88.2 ± 23.7	18.6 ± 6.9

[a]Rat brain region is hippocampus, and the mouse is whole brain.

period. Nevertheless, these ex vivo results confirm that the CsA-induced increase of brain radioactivity seen with PET is due primarily to the parent radioligand itself, with less significant absolute or relative changes in any of the radiometabolites.

DISCUSSION

[^{11}C](*R*)-(−)-RWAY is clearly a substrate for P-gp in rodent brain. In vivo PET imaging and ex vivo tissue radiochromatography showed >2.5-fold increase in brain uptake of radioactivity with pharmacological blockade or genetic inactivation of P-gp. Furthermore, CsA increased the ratio of [^{11}C](*R*)-(−)-RWAY concentrations in brain to plasma, consistent with the localization of this efflux transporter at the blood-brain barrier. Treatment with CsA also caused peripheral effects that might have been interpreted to be the result of P-gp blockade. We examined the effects of CsA on the metabolism of [^{11}C](*R*)-(−)-RWAY and its plasma protein binding.

Radiometabolites in brain and plasma

Radiochromatographic analysis was necessary to monitor composition of brain radioactivity to assess their influence. The measurable amounts of radiometabolites were low and constituted ∼8% of the total radioactivity in rats and ∼13% in mice. The enhanced brain levels of radioactivity after P-gp blockade was mainly due to [^{11}C](*R*)-(−)-RWAY itself. Three distinct radiometabolites were resolved. Because of their uniform distribution in brain, these radiometabolites are probably inactive (i.e., have negligible affinity for the receptor). This approach to identify active vs. inactive metabolites can be applied when the distribution of the target varies among brain regions (Shetty et al., 2006; Zoghbi et al., 2005, 2006).

CsA increased the concentration of radiometabolite C in rat brain, and that metabolite may also be a substrate for P-gp. Nevertheless, the metabolic profile was measured at one time-point (30-min) and may be confounded by CsA-induced changes in the kinetics of metabolism.

In summary, although CsA-enhanced uptake of radioactivity could have been a peripheral metabolic effect, we found that the primary cause was enhanced uptake of the parent radioligand, with a minor contribution from radiometabolite C.

Effect of CsA on plasma free fraction

We found that CsA increased the plasma free fraction of [^{11}C](*R*)-(−)-RWAY in rats, perhaps due to displacement of radioligand from plasma proteins. This effect was substantial, with 2.7-fold increase in f_1. Depending on the radioligand transfer rate into brain and the kinetics of dissociation of plasma protein relative to capillary transit time, brain uptake can be as much as linearly proportional with plasma free fraction. If true for [^{11}C](*R*)-(−)-RWAY, then a sizeable proportion of the increase in brain uptake induced by CsA may actually have been caused by displacement of radioligand from plasma proteins. We measured f_1 of the radioligand at a time of high plasma CsA concentration (i.e., 30 min after its administration), and the 2.7-fold increase of plasma free fraction may not have been sustained for the entire PET scanning session. Nevertheless, this study highlights the importance of examining potential peripheral effects of P-gp blocking drugs on plasma free fraction.

Could pharmacologic doses of the blocking drug WAY 100635 acted like CsA and displaced [^{11}C](*R*)-(−)-RWAY from plasma proteins? We did not examine the possible increase in f_1, but it can occur if the protein binding site is saturable. The primary purpose of the blocking study was to confirm that receptor binding was saturable and reduced brain activity in all regions to uniform levels of nondisplaceable uptake. Our studies confirmed complete displacement (i.e., saturability) of radiotracer binding to the 5-HT$_{1A}$ receptor. An increase of plasma f_1 would increase nonspecific brain uptake. Such an increase is not apparent in Figure 3B but cannot be excluded because of the concurrent clearance of the radiotracer during this experiment with bolus injection of radiotracer. In light of the effects of CsA to increase f_1, examination of the effects of receptor saturating doses of displacing agents should also be considered.

Use of P-gp knockout mice to assess the peripheral effects of CsA

Effects of the CsA-treatment in the P-gp knockout mice should reflect solely the non-P-gp effects of CsA-treatment, since these mice lacking this efflux pump. Brain AUC values of the CsA-treated and the non-treated P-gp knockout mice were indistinguishable and therefore we can assume that CsA demonstrated negligible peripheral effects in the mice. Mice received CsA-treatment at a dose concentration of 25 mg/kg, which is half the dose that the rats received. Mice typically did not survive doses greater than 50 mg/kg.

Receptor occupancy by radioligand

Because of the small size of the rodent brain, a low specific radioactivity of the radioligand can confound imaging results (Jagoda et al., 2004; Kung and Kung, 2005). The nonradioactive ligand can occupy a high enough proportion of the receptors such that *BP* is no longer linear with free concentration or injected radioactivity. We estimated receptor occupancy by comparing the specific uptake (defined as target region minus cerebellum) to published values of 5-HT_{1A} receptor B_{max} (receptor density). Based on an average B_{max} in forebrain of 50 fmol/mg tissue (Flugge et al., 1999), receptor occupancy of specific uptake was <10% for the in vivo studies in rat and mouse. For the ex vivo study of hippocampus, we estimated B_{max} to be 100 fmol/mg tissue, since this region has higher receptor density than the forebrain as a whole. The estimated receptor occupancies for the ex vivo hippocampal measurements were <10% for control animals but ~25% with CsA treatment. Occupancies less than 10% would cause minimal errors in the imaging and direct tissue measurements of *BP*. Nevertheless, the receptor occupancies associated with CsA-treatment for ex vivo (but not in vivo studies) may be problematic. High receptor occupancies by the nonradioactive ligand would be expected to artificially decrease *BP*. That is, receptor binding would begin to saturate and become nonlinear. In fact, the CsA ex vivo values of *BP* were higher than, although not statistically different from, control animals. For example, the hippocampus to cerebellum ratios changed from 5.5 ± 2.6 in controls to 8.2 ± 2.6 after CsA treatment (Fig. 6). Because of the higher receptor occupancy associated with CsA treatment, we have probably underestimated the increase in *BP*, i.e., the true value of *BP* should be >8.2, which has significant implications about how best to quantify 5-HT_{1A} receptor density with [^{11}C](*R*)-(−)-RWAY in rodents.

Implications for receptor quantitation

How should receptor density be quantified if the radioligand is a substrate for P-gp? Compartmental modeling with an arterial input function is commonly regarded as the "gold standard" in PET neuroreceptor imaging. Distribution volume is the outcome measure of compartmental modeling and equals the ratio at equilibrium of radiotracer concentrations in brain and plasma. Thus, if the radioligand is a P-gp substrate, compartmental modeling with arterial input function cannot distinguish changes in receptor density from those that are caused by the activity of P-gp. The complexity of this question can be understood, in part, by considering the proposed mechanism of P-gp. This efflux pump has a preference for lipophilic compounds and is thought to transport them directly from the membrane itself (Gottesman et al., 2002). The drug does not cross the blood brain barrier for subsequent transport from the extracellular domain of brain to the plasma. That is, before the drug completely crosses the endothelial membrane, it is transported back to plasma. In the absence of other identifying information, the effect of P-gp efflux could be equally well modeled by an increase of K_2 (efflux from brain) or a decrease of K_1 (transport to brain). Modeling with standard brain and plasma time-activity curves cannot distinguish these two possibilities. In this situation, the reference tissue input may be the preferred approach. The outcome of such analysis is *BP*, which equals the ratio at equilibrium of specific to nondisplaceable brain radioactivity. If P-gp effects are uniform throughout brain, then this efflux transporter should cause the same percentage effect in specific and nondisplaceable regions, and *BP* should be unchanged. Our results showed that *BP* (i.e., ratio to cerebellum) was much less affected by P-gp blockade than distribution volume (i.e., ratio to radioligand concentration in plasma). Nevertheless, we found a consistent increase in the mean ratios of forebrain to cerebellum radioactivity with CsA blockade in rats and with genetic inactivation of P-gp in mice (Figs. 4 and 6). These results suggest that P-gp is not uniformly distributed in rodent brain and that *BP* as well as distribution volume may be confounded by regionally variable P-gp activity. To estimate these effects in humans, the regional uniformity of P-gp could be examined in monkey brain and even on a pixel-by-pixel basis.

The human *mdr1* (also called *abc b1*) gene that encodes P-gp has several single nucleotide polymorphisms that alter the pharmacokinetics and pharmacodynamics of drugs that are substrates for this transporter (Ieiri et al., 2004; Kurata et al., 2002). The effects of these polymorphisms on radiotracers like [^{11}C]verapamil that are substrates for this transporter are just beginning to be examined (Takano et al., 2006).

CONCLUSION

We used both pharmacologically treated rats and transgenic mice to examine the role of P-gp as an efflux transporter of [^{11}C](*R*)-(−)-RWAY. Although this radioligand is clearly a P-gp substrate in rodents, we recommend care be used to examine peripheral effects of P-gp inhibitors, such as metabolism and plasma protein binding, to isolate those effects that are mediated by P-gp itself at the blood-brain barrier.

ACKNOWLEDGMENTS

The authors thank Mr. Michael Green and Dr. Jurgen Seidel for building the ATLAS PET camera; and Drs. Masao Imaizumi, Fumihiko Yasuno, Ms. Vanessa Cropley, Ms. Lisa Nichols and Mr. Jonathan Gourley for assistance with the rodent imaging.

REFERENCES

Ambudkar SV, Dey S, Hrycyna CA, Ramachandra M, Pastan I, Gottesman MM. 1999. Biochemical, cellular, and pharmacological aspects of the multidrug tranporter. Annu Rev Pharmacol Toxicol 39:361–398.

Ambudkar SV, Kimchi-Sarfaty C, Sauna ZE, Gottesman MM. 2003. P-glycoprotein: From genomics to mechanism. Oncogene 22:7468–7485.

Dagenais C, Graff CL, Pollack GM. 2004. Variable modulation of opioid brain uptake by P-glycoprotein in mice. Biochem Pharmacol 67:269–276.

Doige CA, Ames GFL. 1993. ATP-dependent transport systems in bacteria and humans—Relevance to cystic fibrosis and multidrug resistance. Annu Rev Microbiol 47:291–319.

Flügge G, Pfender D, Rudolph S, Jarry H, Fuchs E. 1999. 5HT$_{1A}$-receptor binding in the brain of cyclic and ovariectomized female rats. J Neuroendocrinol 11:243–249.

Gandelman M, Baldwin RM, Zoghbi SS, Zea-Ponce Y, Innis RB. 1994. Evaluation of ultrafiltration for the free fraction determination of SPECT radiotracers: β-CIT, IBF, and iomazenil. J Pharm Sci 83:1014–1019.

Gottesman MM, Fojo T, Bates SE. 2002. Multidrug resistance in cancer: Role of ATP-dependent transporters. Nat Rev Cancer 2:48–58.

Ichise M, Liow JS, Lu JQ, Takano T, Model K, Toyama H, Suhara T, Suzuki K, Innis RB, Carson RE. 2003. Linearized reference tissue parametric Imaging methods: Application to [^{11}C]DASB positron emission tomography studies of the serotonin transporter in human brain. J Cereb Blood Flow Metab 23:1096–1112.

Ieiri I, Takane H, Otsubo K. 2004. The MDR1 (ABCB1) gene polymorphism and its clinical implications. Clin Pharmacokinet 43: 553–576. Review.

Jagoda EM, Vaquero JJ, Seidel J, Green MV, Eckelman WC. 2004. Experiment assessment of mass effects in the rat: Implications for small animal PET imaging. Nucl Med Biol 31:771–779.

Johnson CA, Seidel J, Vaquero JJ, Pascau J, Desco M, Green MV. 2002. Exact positioning for OSEM reconstructions on the ATLAS depth-of-interaction small animal scanner. Mol Imaging Biol 4: S22 (abstract).

Kung MP, Kung HF. 2005. Mass effect of injected dose in small rodent imaging by SPECT and PET. Nucl Med Biol 32:673–678.

Kurata Y, Ieiri I, Kimura M, Morita T, Irie S, Urae A, Ohdo S, Ohtani H, Sawada Y, Higuchi S, Otsubo K. 2002. Role of human MDR1 gene polymorphism in bioavailability and interaction of digoxin, a substrate of P-glycoprotein. Clin Pharmacol Ther 72:209–219.

Liow J, Seidel J, Johnson CA, Toyama H, Green MV, Innis RB. 2003. A single slice rebinning/2D exact positioning OSEM reconstruction for the NIH ATLAS small animal PET scanner. J Nucl Med 44:162P (abstract). McCarron JA, Chin FT, Pike VW, Hong J, Musachio JL, Ichise M, Zoghbi SS, Vines DC, Vermeulen ES, Wikstrom HV, Halldin C, Innis RB. 2004. New candidate PET radioligand for brain 5-HT1A receptors based on 2,3,4,5,6,7-hexahydro-1{4-[1[4-(2-methoxyphenyl)-piperazinyl]]-2-phenylbutyryl}-1H-azepine (RWAY). Neuroimage 222 (Suppl):T34–T35.

Moochala SM, Renton KW. 1986. Inhibition of hepatic microsomal drug metabolism by the immunosuppressive agent cyclosporin A. Biochem Pharmacol 35:1499–1503.

Passchier J, van Waarde A, Doze P, Elsinga P, Vaalburg W. 2000. Influence of P-glycoprotein on brain uptake of [^{18}F]MPPF in rats. Eur J Pharmacol 407:273–280.

Passchier J, Bender D, Mattews JC, Lawrie KW, Gee AD. 2003. [^{11}C]Loperamide: A novel and sensitive PET probe for quantification of changes in P-glycoprotein functionality. Mol Imaging Biol 5:121 (abstract).

Paxinos G, Watson C. 1998. The rat brain in stereotaxic coordinates, 4th ed. San Diego: Academic Press.

Paxinos G, Franklin KBJ. 2001. The mouse brain in stereotaxic coordinates, 2nd ed. San Diego: Academic Press.

Sadeque AJ, Wandel C, He H, Shah S, Wood AJ. 2000. Increased drug delivery to the brain by P-glycoprotein inhibition. Clin Pharmacol Ther 68:231–237.

Schinkel AH, Smit JJM, Vantellingen O, Beijnen JH, Wagenaar E, Vandeemter L. Mol CA, van der Valk MA, Robanus-Maandag EC, te Riele HP, Berns AJ, Borst P. 1994. Disruption of the mouse mdr1a P-glycoprotein gene leads to a deficiency in the blood-brain barrier and to increased sensitivity to drugs. Cell 77:491–502.

Schinkel AH, Wagennar E, Mol CAAM, van Deemter L. 1996. P-glycoprotein in the blood-brain barrier of mice influences the brain penetration and pharmacological activity of many drugs. J Clin Invest 97:2517–2524.

Seidel J, Vaquero JJ, Green MV. 2003. Resolution uniformity and sensitivity of the NIH ATLAS small animal PET scanner: Comparison to simulated LSO scanners without depth-of-interaction capability. IEEE Trans Nucl Sci 50:1347–1350.

Shetty UH, Zoghbi SS, Liow J-S, Ichise M, Hong J, Musachio JL, Halldin C, Seidel J, Innis RB, Pike VW. 2006. Identification and regional distribution in rat brain of radiometabolites of the dopamine transporter PET radioligand, [^{11}C]PE2I. Eur J Nucl Med Mol Imaging (in press).

Takano A, Kusuhara H, Suhara T, Ieiri I, Morimoto T, Lee YJ, Maeda J, Ikoma Y, Ito H, Suzuki K, Sugiyama Y. 2006. Evaluation of in vivo P-glycoprotein function at the blood-brain barrier among MDR1 gene polymorphisms by using 11C-Verapamil. J Nucl Med 47:1427–1433.

Wacher VJ, Silverman JA, Zhang Y, Benet LZ. 1998. Role of P-glycoprotein and cytochrome P450 3A in limiting oral absorption of peptides and peptidomimetics. J Pharm Sci 87:1322–1330.

Zoghbi SS, Shetty UH, Ichise M, Liow J-S, Hong J, Musachio JL, Seneca N, Halldin C, Seidel J, Pike VW, Innis RB. 2005. The dopamine transporter probe [^{11}C]PE2I shows active and inactive radioactive metabolites in rat brain. J Labelled Comp Radiopharm 48:S98.

Zoghbi SS, Shetty UH, Ichise M, Fujita M, Imaizumi M, Liow J-S, Shah J, Musachio JL, Pike VW, Innis RB. 2006. PET Imaging of the dopamine transporter with ^{18}F-FECNT: A polar radiometabolite confounds brain radioligand measurements. J Nucl Med 47: 520–527.